The Journal of Immunology

# CD23 Trimers Are Preassociated on the Cell Surface Even in the Absence of Its Ligand, IgE



Michelle A. Kilmon, Anne E. Shelburne, Yee Chan-Li, Kevin L. Holmes and Daniel H. Conrad

*J Immunol* 2004; 172:1065-1073; ;
doi: 10.4049/jimmunol.172.2.1065
http://www.jimmunol.org/content/172/2/1065



*The Journal of Immunology* is published twice each month by
The American Association of Immunologists, Inc.,
1451 Rockville Pike, Suite 650, Rockville, MD 20852

Print ISSN: 0022-1767 Online ISSN: 1550-6606.

# CD23 Trimers Are Preassociated on the Cell Surface Even in the Absence of Its Ligand, IgE[1]

**Michelle A. Kilmon,[2]* Anne E. Shelburne,* Yee Chan-Li,* Kevin L. Holmes,† and Daniel H. Conrad[3]***

**Allergic disease is mediated by high levels of allergen-specific IgE. IgE binding to CD23, the low affinity receptor for IgE, results in a negative feedback signal leading to a decrease in IgE production. Previous studies have shown that CD23 associates as an oligomer and that cooperative binding of at least two lectin domains is required for high affinity IgE binding to CD23. We have previously shown that cooperative binding is required for regulation of IgE production. This study describes the production of several mAbs that bind the stalk region of murine CD23. One of the Abs, 19G5, inhibited the IgE/CD23 interaction at 37°C, but not at 4°C. Analysis of the binding properties of these Abs revealed that CD23 dissociates at high temperatures, such as 37°C; however, the N terminus is constitutively associated, indicating partial, rather than complete, dissociation. A novel finding was that the stalk region, previously thought to mediate trimer association, was not required for oligomerization. These data reveal important information about the structure of CD23 that may be useful in modulating IgE production.** ***The Journal of Immunology,*** **2004, 172: 1065–1073.**

CD23 is the low affinity receptor for IgE. It is most known for its role as a negative regulator of IgE production. Mice deficient in CD23 tend to have higher levels of IgE after Ag stimulation, whereas animals overexpressing CD23 produce significantly lower amounts of IgE in response to the same treatments (1–5). Mice transgenic for soluble recombinant extracellular CD23 (sCD23)[4] exhibited no phenotype suggesting that membrane-bound CD23 is responsible for regulating IgE levels (4). CD23 also plays a role in enhancing Ag processing and presentation to T cells. Ag is targeted to CD23 in the form of IgE/Ag complexes, thereby increasing Ag uptake, which leads to enhanced processing and presentation of that Ag (6, 7).

Unlike all other FcRs, which are all members of the Ig superfamily, CD23 has a C-terminal lectin domain, making it a member of the C-type lectin family. This domain is the site of interaction with the Cε3 domain of IgE, and as in other members of this family, the binding of IgE to CD23 is calcium dependent (8–10). The lectin domain is followed by a stalk region (discussed in more below), a transmembrane region, and a very short cytoplasmic domain.

CD23 is initially expressed as a membrane-bound molecule, but is then cleaved by an unknown protease, releasing the majority of the protein. CD23 is cleaved at several sites within the stalk region, resulting in fragments of different sizes, all of which contain the lectin domain. All soluble fragments in mice and humans, except the 12-kDa fragment, can bind IgE, but with only a low affinity (11, 13).

Beavil et al. (14) noticed a periodic seven-amino acid repeat throughout the length of the stalk region of CD23. Almost every seventh position contains a leucine or other hydrophobic amino acid, suggesting that CD23 could form an α-helical coiled coil (14). Molecular modeling of CD23 as well as cross-linking data suggested that CD23 would form a trimer instead of a dimer, which is normally seen with proteins containing leucine zippers (14, 15). The use of reversible cross-linkers showed that only the 49-kDa form of CD23 was present in the oligomers (15). Scatchard analysis showed that IgE binds CD23 with a dual affinity; both a high affinity ($K_a$ = 4–10 × $10^7$ $M^{-1}$) and a low affinity ($K_a$ = 4–10 × $10^6$ $M^{-1}$) binding component were seen (15). To explain these data, Gould et al. (16) suggested a model in which CD23 forms trimers, and oligomerization of CD23 mediates high affinity binding to IgE. Oligomerization of CD23 would allow the lectin domains to come within close proximity of each other and to cooperate in binding one IgE molecule, resulting in high avidity binding.

Several studies have shown that Abs that bind to CD23 can modulate IgE production. Sherr et al. (17) were the first to demonstrate that anti-CD23 has the ability to inhibit IgE production, and a number of additional studies have confirmed this finding both in vivo and in vitro (18–20). One of the most recent studies demonstrated that the ε germline transcript is inhibited, suggesting that the mechanism involves inhibition of isotype switching (21). In contrast, Abs that bind the stalk promote an increase in IgE levels in vivo and in vitro (19, 22). One of these Abs, a polyclonal anti-stalk, inhibited high affinity IgE binding to murine CD23 while having no effect on low affinity binding, suggesting that Abs that bind to the stalk prevent the cooperative association of the lectin domains required for high affinity IgE binding (22). To examine this phenomenon in more detail, we produced several anti-stalk mAbs against the mouse stalk. We found that CD23 is preassociated on the cell surface in the absence of ligand. We observed that under physiological conditions, CD23 is partially

*Department of Microbiology and Immunology, Virginia Commonwealth University, Richmond, VA 23298; and †Flow Cytometry Section, National Institute of Allergy and Infectious Disease, National Institutes of Health, Bethesda, MD 20892

Received for publication May 7, 2003. Accepted for publication November 4, 2003.

The costs of publication of this article were defrayed in part by the payment of page charges. This article must therefore be hereby marked *advertisement* in accordance with 18 U.S.C. Section 1734 solely to indicate this fact.

[1] This work was supported by Grants AII8697 and AI44163 from the U.S. Public Heath Service. M.A.K. was supported in part by National Institute of Allergy and Infectious Diseases Training Grant AI07407.

[2] Current address: Department of Microbiology and Immunology, University of North Carolina, CB Number 7290, Chapel Hill, NC 27599.

[3] Address correspondence and reprint requests to Dr. Daniel H. Conrad, Department of Microbiology and Immunology, Virginia Commonwealth University, Box 980678, MCV Station, Richmond, VA 23298. E-mail address: dconrad@hsc.vcu.edu

[4] Abbreviations used in this paper: sCD23, soluble recombinant extracellular CD23; CD40LT, recombinant CD40 ligand trimer; CFP, cyan fluorescent protein; FRET, fluorescence resonance energy transfer; ΔR2, a mutant of CD23 lacking three of the 21 heptad repeats; YFP, yellow fluorescent protein.



0022-1767/04/$02.00

dissociated; only the upper portion of the molecule, including the lectin domain, dissociates. We also determined that the stalk region, which has been previously thought to mediate oligomerization of CD23, is not required for CD23 to associate as trimers. Only the transmembrane and cytoplasmic regions are required for association to occur. This suggests that the role of the stalk is to direct the correct orientation of the lectin heads needed for high affinity IgE binding to occur while either the transmembrane or the cytoplasmic region controls trimerization of the receptor.

## Materials and Methods

### *Reagents and animals*

Baculovirus supernatant containing recombinant murine IL-4 was a gift from Dr. W. Paul (National Institutes of Health, Bethesda, MD). Recombinant murine IL-5 was purchased from R&D Systems (Minneapolis, MN). Recombinant CD40 ligand trimer (CD40LT) (23) and M15 (mouse IgG1 anti-CD40 ligand trimer) were obtained from Immunex (Seattle, WA) (23). FITC-anti-CD23 (B3B4), which is an anti-lectin mAb (12), was obtained from BD PharMingen (San Diego, CA). Rat IgE (IR162) (24) and monoclonal mouse IgE (mIgE-DNP) (25) from H1-DNP-ϵ-26 were purified from ascites as described previously (26). 2H10 (27), an anti-CD23 lectin mAb, and C0H2, a rat IgG2a used as an isotype control Ab, were also purified from ascites. Mouse IgE, rat IgE, and 19G5 were labeled with [$^{125}$I]NaI (NEN Life Science, Boston, MA) using the chloramine T method as previously described (28). Abs were biotinylated with a 100-fold molar excess of EZ-link Sulfo-NHS-biotin (Pierce, Rockford, IL) in PBS/10 mM HEPES. BALB/c mice and LouM rats were purchased from the National Cancer Institute (Fredrick, MD). All animals used in experiments were between 6 and 10 wk of age and were kept in an accredited animal facility.

### *Production of anti-stalk mAbs*

LouM rats were injected with 200 $\mu$g of mouse stalk protein emulsified in CFA (22). The rats were boosted twice with 200 $\mu$g of stalk protein emulsified in IFA. Serum Ab titers were tested by ELISA. Spleen cells from the immunized rats were fused to IR983F myeloma cells (29) as described previously, except that a ratio of two spleen cells per myeloma cell was used (12). A fusion of the rat spleen cells and the mouse myeloma, P3×63-AG8.653, was performed by the Hybridoma Core Facility (Virginia Commonwealth University) using the protocol described by Kohler and Milstein (30). Colonies that emerged from these fusions were tested for reactivity to mouse stalk by ELISA. ELISA plates were coated with 5 $\mu$g/ml recombinant stalk protein, and the samples were detected using goat anti-rat Ig-AP (Southern Biotechnology Associates, Birmingham, AL). Positive colonies were single-cell-cloned by limiting dilution. Five clones were identified that remained positive for mouse stalk; 2E4, 19G5, and 4B8 were produced from the rat-rat fusions, and 1F3 and 2B9 were produced from the rat-mouse fusion. The isotype of each of the Abs was determined using a kit from BD Biosciences (Palo Alto, CA). Ascites was prepared in LouM rats (rat-rat fused cells) or nude mice (rat-mouse fused cells), and the Abs were purified by ammonium sulfate precipitation and a combination of ion exchange and gel filtration as previously described (12) or by protein G affinity chromatography according to the manufacturer's instructions (Amersham Pharmacia Biotech, Piscataway, NJ).

The region of CD23 to which the anti-stalk Abs bound was determined by ELISA. ELISA plates were coated with 5 $\mu$g/ml of the full-length *lz*-ECCD23 (extracellular CD23 containing an N-terminal modified leucine zipper motif) or mutants lacking part of the stalk (27). After 1-h incubation at 37°C, the plates were blocked with PBS containing 2 mM $CaCl_2$, 10 mM HEPES (pH 7.4), 150 mM NaCl, 1% FBS, and 0.02% Tween 20. This was followed by addition of biotinylated mAbs starting at 20 $\mu$g/ml and diluted 1/2 across the plate. Binding of the mAbs was detected using a goat anti-biotin-HRP (Vector Laboratories, Burlingame, CA), followed by TMB substrate (DAKO, Carpinteria, CA). The plates were read at a wavelength of 450 nm after stopping the reaction using 0.18 M sulfuric acid.

### *Cell culture and B cell preparation*

293T, a human kidney endothelial cell line (gift from D. McVicar (National Cancer institute, Frederick, MD)), was used for transient transfection of cyan fluorescent protein (CFP) and yellow fluorescent protein (YFP) fusion proteins, and was grown in complete DMEM (10% FBS (HyClone, Logan, UT), 100 U/ml penicillin and streptomycin, and 2 mM L-glutamine (both purchased from Life Technologies, Gaithersburg, MD)). Chinese hamster ovary cells (CHO-K1) were obtained from American Type Culture Collection (Manassas, VA) and were maintained in complete DMEM. CD23 expressing CHOK1 cells, Fc1.7, were made as previously described and grown in DMEM-GS (15). Resting B cells were purified as previously described (32, 33). To examine the effect of the anti-stalk mAbs on CD23 cleavage, $5 \times 10^5$ Fc1.7 cells or purified B cells stimulated with IL-4 and CD40LT as previously described (22) were cultured for 18 h in the presence of the indicated concentration of 19G5, 11B4, 17G9, or C0H2. The amount of CD23 on the cell surface was determined by FACS analysis, and sCD23 release was measured by ELISA (34).

### *Scatchard plots and binding assays*

The affinity of IgE for CD23 with or without the presence of 19G5 or 2H10 was determined as previously described (22). Scatchard analysis was used to determine the affinities of 19G5, 2B9, and 2H10 for CD23. Fc1.7 cells or CHO cells ($6 \times 10^5$) were allowed to equilibrate to the indicated temperature, after which they were incubated with increasing concentrations of $^{125}$I-labeled mAb (0.5–8 $\mu$g/ml) for 75 min. The cells were then spun over a phthalate oil mixture (35) to separate the unbound mAb. Specific binding to CD23 was determined by subtracting the counts per minute of the CHO cells incubated with $^{125}$I-labeled mAb from the counts per minute of FC1.7 cells incubated with $^{125}$I-labeled mAb. Binding affinities were determined by linear regression analysis. Inhibition of IgE binding was determined by incubating $6 \times 10^5$ Fc1.7 cells with increasing concentrations of cold 19G5 or 2H10 (1–166 $\mu$g/ml) for 1 h at the indicated temperature. [$^{125}$I]IgE (300 ng) was then added, and the cells were allowed to incubate for another hour before being spun through a phthalate oil mixture. Specific binding was determined by subtracting the counts per minute of cells incubated with a 100-fold excess of cold IgE. The percent inhibition was calculated as follows: (cpm of cells with Ab added/cpm of untreated cells) × 100. Dissociation of CD23 from IgE was performed by incubating Fc1.7 cells with [$^{125}$I]IgE (5 $\mu$g/ml) for 1 h at the appropriate temperature, after which a 100-fold excess of IgE, 19G5, or 2H10 was added. At the indicated times, the cells were spun over phthalate oil to determine the amount of IgE bound. The percent bound was calculated as follows: (cpm of cells with Ab added/cpm of untreated cells) × 100.

### *Production and expression of CD23 CFP and YFP fusion proteins*

The CD23 cDNA was transferred into pECFP-C1 and pEYFP-C1 (both from Clontech, Palo Alto, CA) by PCR using primers that added a 5′ *Sal*I site (GTCACGGATCCATGGA-AGAAAATGAATACTCAGG) and a 3′ *Hpa*I site (GTTAACTCTTCTGAGATGAG-TTTTTGTTCGAAGGG). This produced CD23 with either a CFP or YFP in-frame at the N terminus, depending on the vector (CD23-pECFP-C1 and CD23-pEYFP-C1). A CD23 deletion mutant lacking aa 88–107 in the stalk region (ΔR2) (15) was also inserted into the pEYFP-C1 and pECFP-C1 vectors so that the CFP and YFP were in-frame with Δ88–107 at the N terminus (Δ88–107-pECFP-C1 and Δ88–107-pEYFP-C1). This was also performed by PCR using the same 5′ primer as that used above and a primer that added a 3′ *Hpa*I site (GTTAACCCTCGAGATCCATTGTGAGCAGAAG). A truncation mutant (Mut1) was made by inserting a stop codon just after the transmembrane region at base 327 in the cDNA using the Quickchange method (Stratagene, La Jolla, CA) according to the manufacturer's directions. The mutation was first made in CD23-pECFP-C1 with the following oligonucleotides: 5′ (GGAAACGGAGAAGAATTGAAAACAGCTGG GAG) and 3′ (CTCCCAGCTGT-TTTCAATTCTTCTCCGTTTCC; mutated bases are underlined). The truncated CD23 was then transferred into pEYFP-C1 using the *Sal*I and *Hpa*I restriction endonuclease sites added in the original PCR of CD23 above. Control vectors containing FAS-CFP, FAS-YFP, and CFP-YFP fusion proteins (36) were gifts from Dr. M. J. Lenardo (National Institutes of Health, Bethesda, MD). The CFP and YFP fusion proteins were transfected into 293T cells using Fugene 6 (Roche, Indianapolis, IN) according to the manufacturer's instructions.

### *Fluorescence resonance energy transfer (FRET)*

293T cells were transfected with Fugene according to the manufacturer's directions with 1 $\mu$g of plasmid, except when CFP and YFP vectors were transfected together and then 0.5 $\mu$g of the CFP vector was used. A CFP-YFP fusion protein (37) was used as a positive control, and FAS-$CFP_{1–140}$ and FAS-YFP (36) were transfected along with the CD23-YFP and CD23-CFP fusion proteins as negative controls. Cells transfected with CFP and YFP vectors were analyzed using a FACSVantage SE flow cytometer (BD Immunocytometry Systems, Mountain View, CA) as previously described (38, 39). Briefly, direct excitation of YFP was detected in FL1 (P3) using a 514-nm argon laser at laser position 1; emission of CFP is detected in FL5 (P6), and YFP emission due to FRET was detected in FL4 (P5) using a 413-nm krypton laser at laser position 2. As FRET is sensitive to donor/

Table I. *Description of anti-stalk monoclonal antibodies*[a]

| mAb | Region of Binding | Isotype | L Chain | Binding to CD23 Mutants | | | |
|---|---|---|---|---|---|---|---|
| | | | | Full-length | aa 86-331 | aa 108-331 | aa 139-331 |
| 19G5 | Stalk | $IgG_{2a}$ | κ | + | + | + | − |
| 2E4 | Stalk | $IgG_1$ | κ | + | + | − | − |
| 4B8 | Stalk | $IgG_1$ | κ | + | + | − | − |
| 1F3 | Stalk | IgM | κ | + | + | − | − |
| 2B9 | Stalk | $IgG_1$ | κ | + | + | − | − |
| 2H10 | Lectin | $IgG_{2a}$ | λ | + | + | + | + |

[a] The isotype of both the H and L chains of each mAb was determined by ELISA. The epitope on CD23 where each of the mAbs bound was determined by ELISA using *lz*-ECCD23 deletion mutants (27) that are lacking part of the stalk region. +, binding, −, lack of binding.

acceptor ratios (40), several different ratios of CD23-YFP and CD23-CFP were examined, and the highest FRET values were obtained at a 2/1 ratio (YFP/CFP, respectively; data not shown). Thus, FRET experiments were performed with YFP in excess of CFP (2/1 molar ratio). The data was analyzed using WinMDI (The Scripps Institute, La Jolla, CA). The CFP-positive population was gated for the determination of FRET in histogram analyses.

## Results

*Production of mAbs against the stalk region of mouse CD23*

To examine the role the stalk region of CD23 plays in IgE binding, five mAbs were produced by fusing splenocytes from rats immunized with mouse stalk protein (22) with either a rat or a mouse myeloma. Binding of the mAbs to CD23 was confirmed by both ELISA and Western analysis (data not shown). The region of CD23 to which the anti-stalk Abs bound was determined by ELISA using a series of chimeric CD23 molecules in which portions of the stalk region were deleted (31). These data are summarized in Table I. Four of the anti-stalk Abs (2E4, 4B8, 1F3, and 2B9) recognized epitopes close to the transmembrane in the region of aa 86–107, and one, 19G5, bound in the region of aa 108–139 near the middle of the stalk. An anti-lectin mAb, 2H10, bound each of the CD23 mutants. A schematic of the relative binding sites of the mAbs is shown in Fig. 5*E*.

*Effect of the anti-stalk Abs on CD23 cleavage*

We previously described a polyclonal rabbit anti-CD23 stalk Ab, RAS1, that stabilizes CD23 on the cell surface (22). To determine whether binding of the anti-stalk mAb to CD23 influenced proteolysis of CD23, CD23-expressing CHO cells, Fc1.7, were cultured overnight in the presence of each of the mAbs. Only one of the mAbs, 19G5, had any significant effect on CD23 cleavage. CD23 surface levels were significantly lower after culture with 19G5 (Fig. 1*A*). We also tested the effect of 19G5 binding to CD23 on murine B cells. In the presence of 19G5, CD23 surface levels on IL-4-and CD40L-stimulated B cells were decreased in a dose-dependent manner (Fig. 1*B*), and correspondingly, sCD23 levels were increased (Fig. 1*C*).

*The anti-stalk mAb, 19G5, inhibits IgE binding to CD23*

We determined the capacity of 19G5 to inhibit IgE binding to CD23. Increasing concentrations of 19G5 were incubated with CD23-expressing CHO cells at different temperatures for 1 h, followed by [$^{125}$I]IgE for 1 h. At the lower temperatures (4 and 15°C), 19G5 did not significantly inhibit IgE binding (Fig. 2). However, at higher temperatures, 19G5 did inhibit IgE binding to CD23. At 25°C, 200 μg/ml 19G5 inhibited IgE binding ~40%, whereas the same concentration exhibited 100% inhibition at 37°C. Conversely, an anti-lectin mAb, 2H10, completely inhibited IgE binding to CD23 at both low and high temperatures (4°C data are shown in Fig. 2). Inhibition of IgE binding by the other anti-stalk mAbs was tested at 37°C. 4B8 was the only other Ab to inhibit IgE binding. However, <40% inhibition was seen with 200 μg/ml 4B8 (data not shown).

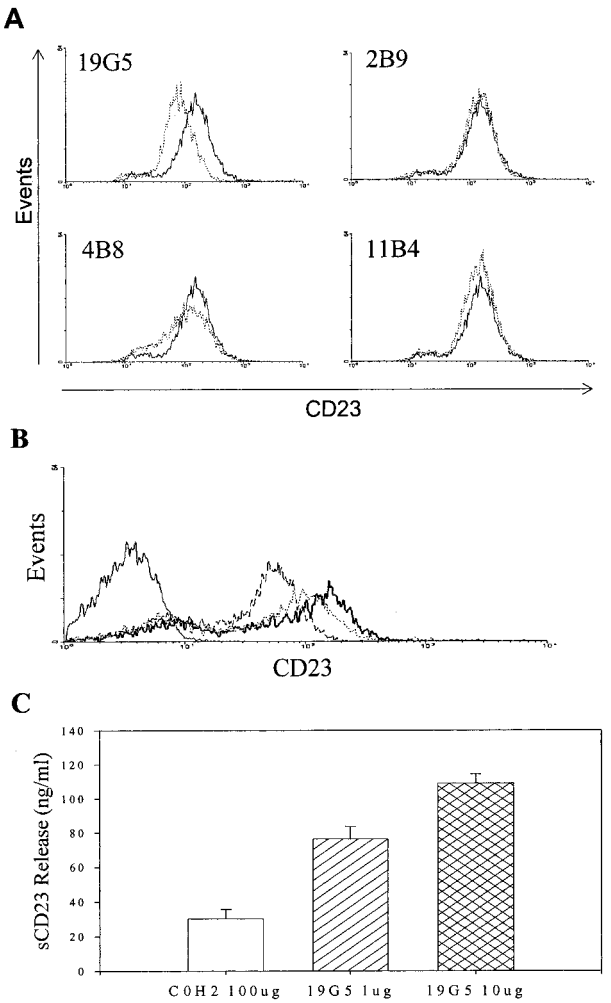


**FIGURE 1.** CD23 proteolysis is enhanced by the mAb 19G5. *A*, Fc1.7 cells were cultured overnight with 100 μg/ml 19G5, 2B9, 4B8, or 11B4. The cells were then harvested, and CD23 surface levels were determined by FACS analysis. The solid line represents CD23 levels in cells not treated with mAb, and the dotted line represents the level of CD23 after mAb treatment. *B*, Resting B cells were stimulated with IL-4 and CD40LT and then cultured in the presence of 100 μg/ml C0H2 (thick line), 10 μg/ml 19G5 (dashed line), or 1 μg/ml 19G5 (dotted line) for 18 h. The cells were harvested and stained for CD23 surface expression. The thin line represents unstained cells. *C*, Supernatants from these cultures were tested for sCD23 release by ELISA. Error bars represent ±1 SE. **, $p < 0.01$.

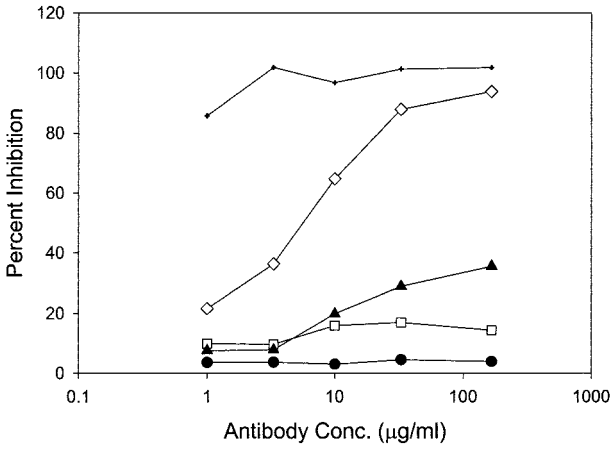


**FIGURE 2.** 19G5 inhibits IgE binding to CD23 more effectively at higher temperatures. The indicated concentrations of 19G5 were allowed to prebind Fc1.7 cells at 4°C (●), 15°C (□), 25°C (▲), or 37°C (◇) for 1 h, followed by incubation with $^{125}$I-labeled IgE. 2H10 was also used, and binding was performed at 4°C (+). Cell-bound IgE was determined after 1 h in duplicate aliquots of cells. Inhibition of IgE binding is shown as the percent inhibition compared with the IgE control.

We previously reported that RAS inhibited high affinity IgE binding to CD23 while having no effect on low affinity IgE binding (22). Using saturation analysis, we determined that the mAb 19G5 also inhibited only high affinity IgE binding to CD23 (Fig. 3). As expected 2H10, an mAb that binds to the lectin head of CD23 at an epitope very close to the site where IgE binds, inhibited both high and low affinity IgE binding to CD23 (Fig. 3).

*19G5 influences IgE dissociation at 37°C only*

A previous report demonstrated that the dissociation rate of IgE from CD23 is much faster at 37°C than at 4°C (23 min vs 3 h, respectively) (41). Dissociation of IgE is performed by allowing [$^{125}$I]IgE to bind to CD23 until it reaches equilibrium. Then a 100-fold excess of cold IgE is added. Samples are taken at multiple time points, and the amount of [$^{125}$I]IgE bound to the cells is determined. We wanted to compare the effects of both the anti-stalk and anti-lectin mAbs on IgE dissociation from CD23. This was performed by adding a 100-fold excess of either 19G5 or 2H10 instead of IgE. In the presence of either 19G5 or 2H10, IgE was readily dissociated at 37°C, although the rate of dissociation was somewhat slower with the mAbs than with IgE itself (Fig. 4*B*). At 4°C, 2H10 caused dissociation of IgE from CD23 at a rate slower than IgE, whereas 19G5 had no effect on IgE dissociation (Fig. 4*A*). This is indicative that both mAbs inhibit binding of IgE not by directly competing for the binding site, but either by steric inhibition or by preventing association of the trimer, thereby inhibiting IgE binding. The latter is most likely the case for 19G5, although either possibility cannot be ruled out for 2H10.

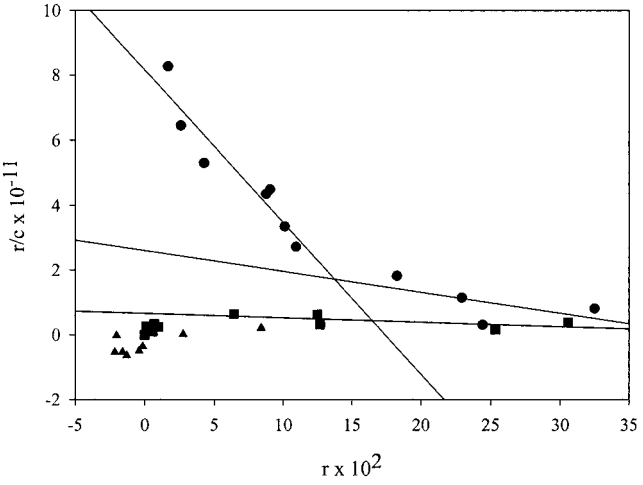


**FIGURE 3.** Like RAS1, 19G5 inhibits high affinity IgE binding while having no effect on low affinity IgE binding. Fc1.7 cells were incubated with increasing concentrations of cold IgE alone (●) or in the presence of 19G5 (■) or 2H10 (▲) for 1 h, followed by $^{125}$I-labeled IgE. After 1 h, cell-bound counts per minute were determined on duplicate aliquots of cells. The lines represent regression analysis for binding in the presence of 19G5 or 2H10; no line was drawn for 2H10, because all points were in same area, indicating no significant binding above background.

*19G5 binds more epitopes at 37 than at 4°C*

To explore whether temperature has an effect on the structure of CD23, allowing 19G5 to inhibit IgE binding more effectively at a higher temperature, we examined the abilities of several anti-CD23 Abs to bind at both 4 and 37°C. B cells stimulated with IL-4 and

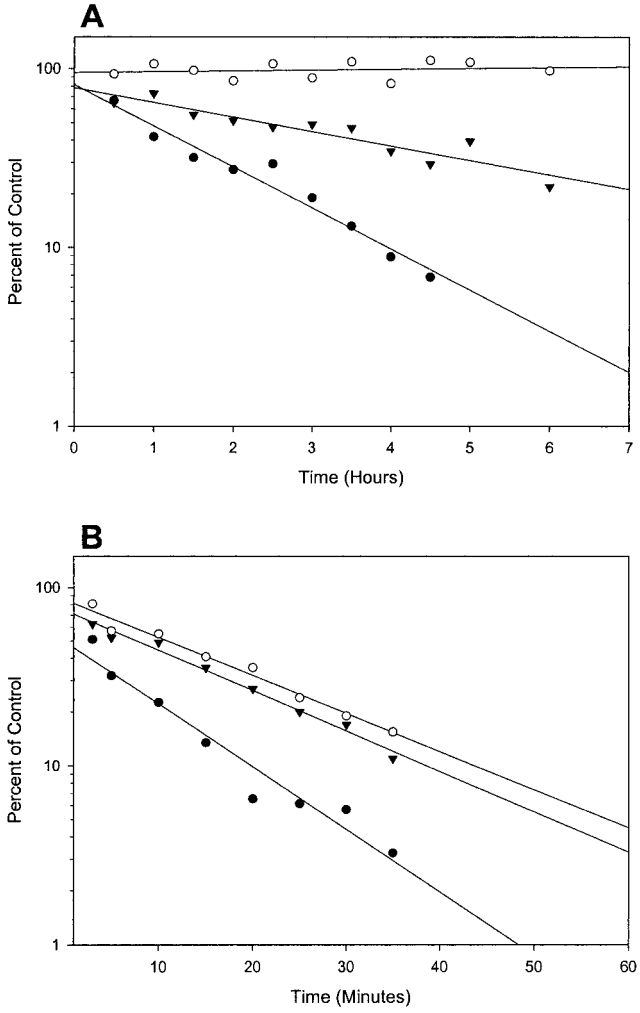


**FIGURE 4.** 19G5 causes dissociation of IgE bound to CD23 at 37°C, but not at 4°C. Fc1.7 cells were equilibrated to either 4°C (*A*) or 37°C (*B*) and then incubated with 5 μg/ml [$^{125}$I]IgE for 1 h, after which a 100-fold excess of IgE (●), 19G5 (○), or 2H10 (▼) was added. At the indicated time points, cells were removed, and the amount of IgE bound was determined and compared with that in cells to which no Ab was added (control). The lines represent regression analysis.

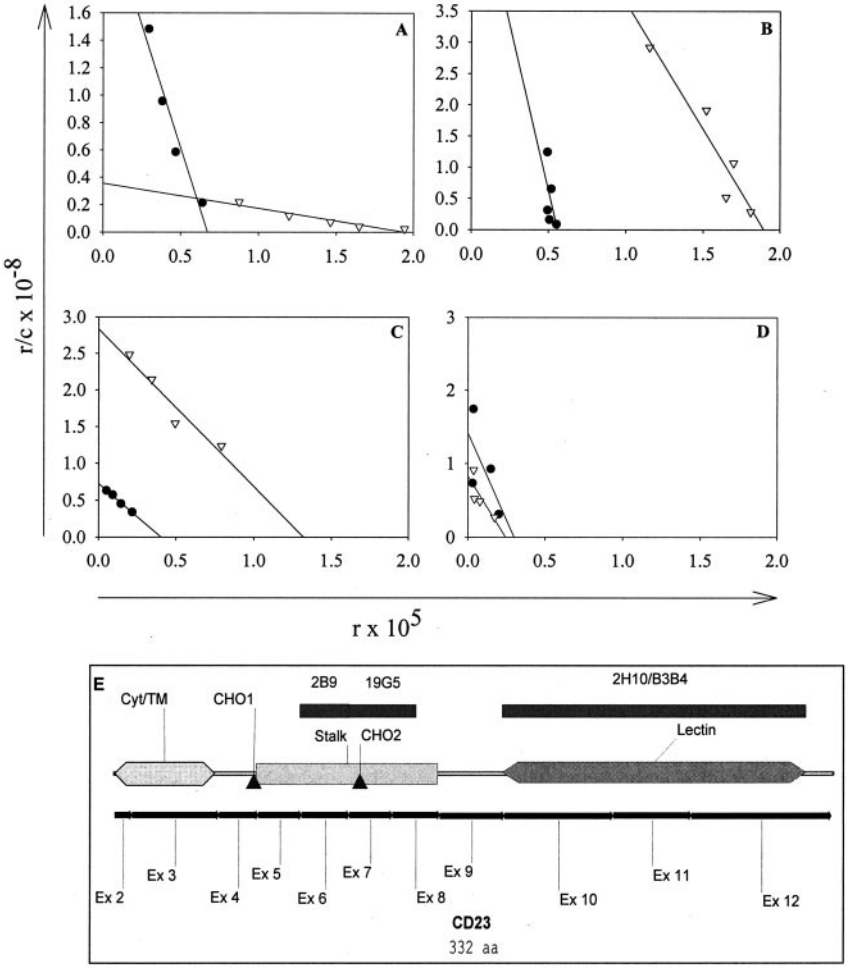


**FIGURE 5.** Scatchard analysis shows that there are more 19G5 and 2H10 binding sites on CD23-positive cells at 37 than at 4°C. $^{125}$I-labeled 2H10 (*B*), 19G5 (*C*), and 2B9 (*D*) cells were allowed to bind Fc1.7 cells for 90 min at 4°C (●) or 37°C (▽). IgE binding (*A*) was determined at 4°C. The counts per minute bound was determined in duplicate aliquots of cells. The lines represent regression analysis. *E*, A schematic of where the epitopes for anti-CD23 epitopes are located, based on the capacity to bind to mutant CD23 molecules (27); also shown are the relative positions of domains and the respective exons that encode the relative regions. The exon data are from Ref. 50.

CD40LT to induce CD23 expression were incubated with each of the anti-stalk mAbs as well as the anti-lectin mAb, 2H10, for 1 h. The amount of mAb bound to the B cell was determined by FACS analysis. Each of the Abs bound to CD23 equally well at 4°C (data not shown). Both 19G5 and 2H10 exhibited more binding to the cells at 37°C. Binding of the anti-stalk mAb, 2B9, did not change significantly with temperature (data not shown).

The exact number of epitopes recognized by 19G5, 2H10, and 2B9 was determined by saturation analysis. At 4 and 37°C, both 19G5 and 2H10 exhibited similar affinities for CD23; however, there was 3 times the number of binding sites for each of the Abs at the higher temperature (Fig. 5 and Table II). 2B9, an anti-stalk mAb that did not inhibit IgE binding, exhibited the same number of binding sites per cell regardless of the temperature, and this number was similar to the number of 19G5 and 2H10 molecules bound at 4°C (Fig. 5 and Table II). There are 3 times the number of low affinity binding sites for IgE as there are high affinity binding sites (Fig. 5 and Table II). Interestingly, the number of binding sites for 19G5 and 2H10 at 4°C and 2B9 at both temperatures is comparable to the number of high affinity IgE binding sites. The number of binding sites for 19G5 and 2H10 at 37°C is similar to the number of low affinity IgE binding sites.

### *Association of CD23 determined by FRET*

FRET was used to further examine the association of CD23. FRET is the radiationless transfer of energy from an excited fluorophore (donor) to another fluorophore (acceptor). Vectors containing the fusion proteins were transfected into 293T cells, and FRET was measured using FACS analysis. The results are shown in Fig. 6. A significant amount of emission at the YFP wavelength was observed when the CD23-CFP/CD23-YFP double-transfected cells were excited through CFP indicating FRET. As a negative control, FAS-CFP and CD23-YFP-C1 (YFP fused to the N terminus of CD23) were cotransfected and examined for FRET. FAS and CD23 would not be expected to associate with each other, because FAS self-associates using a PLAD domain (pre-ligand-binding assembly domain) (42) that CD23 lacks. However, a small amount of FRET was observed in the Fas-CFP/CD23-YFP cotransfected cells. Although the reason for this low level is unclear, the difference between this control (2.7%) and the CD23-CFP/CD23-YFP-

Table II. *The numbers of 19G5 and 2H10 binding sites at 4 and 37°C correspond to the numbers of high and low affinity IgE binding sites*[a]

| | No. of High Affinity Binding Sites | No. of Low Affinity Binding Sites | Low Affinity/ High Affinity Binding Sites |
|---|---|---|---|
| IgE | 67,416 | 197,222 | 2.9 |
| | No. of Binding Sites at 4°C | No. of Binding Sites at 37°C | No. of 37/4°C Binding Sites |
| 2H10 | 56,053 | 189,394 | 3.4 |
| 19G5 | 40,492 | 131,998 | 3.2 |
| 2B9 | 30,000 | 24,553 | .82 |

[a] Numbers were determined from the saturation analyses shown in Fig. 5.

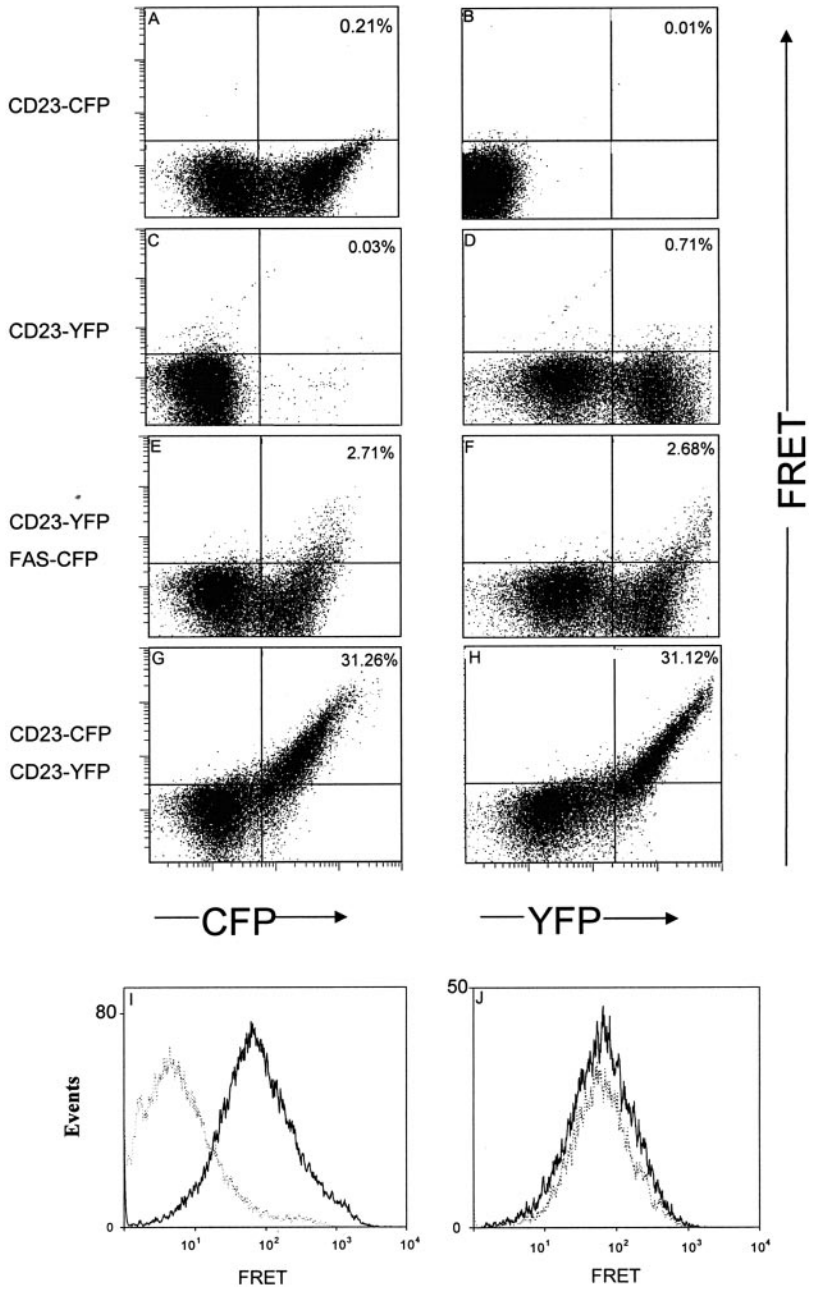


**FIGURE 6.** CD23 is preassociated on the cell surface in the absence of its ligand, IgE. CD23-CFP (*A* and *B*), CD23-YFP (*C* and *D*), CD23-YFP/Fas-CFP (*E* and *F*) or CD23-YFP/CD23/CFP (*G* and *H*) were transfected into 293T cells as indicated and examined for FRET by FACS analysis after 24-h culture. The data are plotted as a dot plot showing the CFP- or YFP-positive cells vs FRET. *I*, The CFP-positive cells shown in the two *right quadrants* of *E* and *G* were gated to analyze the FRET-positive cells by histogram analysis. The solid line represents CD23-CFP/CD23-YFP-transfected cells, and the dotted line represents Fas-CFP-/CD23-YFP-transfected cells. *J*, FRET analysis of CD23-CFP/CD23-YFP-transfected cells at 4°C (dotted line) and 37°C (solid line).

-transfected cells (31%) is obvious, and indeed, essentially all the positive cells exhibited FRET, indicating that all CD23-CFP/CD23-YFP-cotransfected cells examined have coassociated CD23 molecules. FRET analysis by confocal microscopy will be required to determine whether all the CD23 are coassociated, and this has not as yet been completed. The *bottom left* plot shows these data as a histogram, emphasizing the increased FRET seen with the CD23 pair. As indicated in *Materials and Methods* and previously (40), FRET values were sensitive to the donor/acceptor ratio. The results shown were at the indicated 2/1 ratio of YFP to CFP. As a positive control, transfection of Fas-CFP/Fas-YFP, as described previously (36), clearly exhibited FRET (data not shown). We examined whether FRET at the N terminus was influenced by temperature change, binding of IgE, or binding of anti-stalk Abs. The amounts of FRET observed at 4 and 37°C were exactly the same (Fig. 6*J*). Addition of the ligand for CD23, IgE, did not change the amount of FRET observed, nor did binding of the anti-stalk Abs, RAS1 and 19G5 (data not shown). Fig. 7*A* shows a diagram comparing wild-type CD23 to ΔR2. ΔR2, a mutant of CD23, lacks one of the four 21-aa repeats and binds IgE with only low affinity, suggesting that removal of the heptad repeats disrupts oligomerization of CD23 (15). ΔR2 exhibited the same amount of FRET as wild-type CD23 (Fig. 7*B*). All these data suggest that the N terminus remains associated at all times under all conditions.

The requirement of the stalk region for association at the N terminus was determined by creating a CD23 truncation mutant (Mut1). Mut1 was made by inserting a stop codon just between the transmembrane region and the stalk region (Fig. 7*A*). The level of FRET observed at the N terminus was similar to that seen with wild-type CD23, indicating that this region is sufficient for association of CD23 (Fig. 7*C*). Early studies with mouse B cell CD23 had shown no differences in molecular weight when analyzed by SDS-PAGE under reducing and nonreducing conditions, indicating that the cytoplasmic cysteines are not responsible for this association (43).

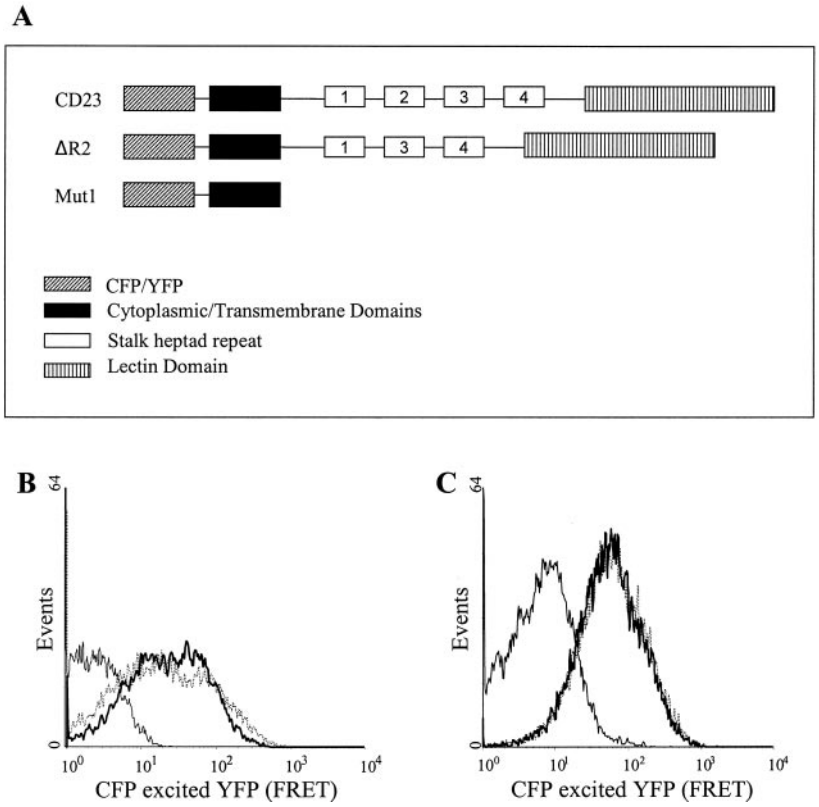


**FIGURE 7.** The stalk region of CD23 is not required for association. The molecules shown in *A* represent the wild-type CD23 and CD23 deletion mutants fused to CFP/YFP and used in the FRET experiments shown in *B* and *C*. *B*, A histogram showing FRET in 293T cells transfected with wild-type CD23-CFP-C1 alone (thin line), wild-type CD23-CFP-C1 and CD23-YFP-C1 (thick line), or ΔR2-CFP-C1 and ΔR2-YFP-C1 (dotted line). *C*, The FRET signal detected in cells transfected with a CD23 truncation mutant, Mut-1-CFP-C1 or Mut-1-YFP-C1 (dotted line), compared with the FRET signals of wild-type CD23-CFP-C1 alone (thin line) and wild-type CD23-CFP-C1 and CD23-YFP-C1 (thick line).

## Discussion

Our laboratory previously described a polyclonal Ab that binds to the stalk region of murine CD23 (22). This Ab, RAS1, inhibited high affinity IgE binding to CD23 while having no effect on low affinity IgE binding, presumably because RAS1 inhibits oligomerization of CD23. To further examine the mechanism by which Abs that bind to the stalk region inhibit high affinity IgE binding, several anti-stalk mAbs were produced. One of the anti-stalk mAbs produced, 19G5, increased CD23 susceptibility to cleavage, resulting in lower CD23 surface expression and increased sCD23 release. This same Ab also inhibited IgE binding to CD23. None of the other anti-stalk mAbs exhibited any significant effect on either CD23 proteolysis or IgE binding. Similar to the polyclonal anti-stalk Ab, 19G5 inhibited only high affinity IgE binding. The low affinity binding also changes somewhat, but this is probably due to a decreased influence from the high affinity component. High affinity binding is presumed to require the cooperative interaction of at least two lectin domains, and low affinity binding would be observed when IgE interacts with only one lectin domain. Interestingly, 19G5 only inhibited IgE binding at high temperatures (25–37°C). Little or no inhibition of IgE binding was seen when 19G5 was allowed to bind to CD23 at low temperatures (4–15°C). This observation led us to examine whether inhibition of IgE binding by the polyclonal Ab was also temperature dependent. Indeed, RAS1 inhibited IgE binding more effectively at 37 than at 4°C (data not shown). These data suggest that there is a physical change in CD23 (most likely dissociation of the trimers) that allows more Ab molecules to bind at 37 than at 4°C. Binding of the Abs to the stalk would prevent proper association of the lectin heads and the cooperative binding required for high affinity IgE binding.

Using epitope mapping, we determined that the mAbs that did not influence IgE binding recognize an epitope on the stalk that is fairly close to the transmembrane region. 19G5 binds an epitope further away from the transmembrane, but only about half-way up the stalk in the region of aa 108–139. This difference suggested that there could be a correlation between the location of binding on the stalk and the ability to inhibit IgE binding. Using FACS analysis we determined that there was more 19G5 binding at 37 than at 4°C, a binding pattern similar to that observed with 2H10, an anti-lectin mAb. The number of binding sites at 37°C correlated to the number of low affinity IgE binding sites, and the number of binding sites observed at 4°C was similar to the number of high affinity IgE binding sites. 2B9, an anti-stalk mAb that did not inhibit IgE binding, bound the same number of sites regardless of temperature. The number of 2B9 binding sites per cell correlated to the number of low affinity IgE binding sites. These data are in agreement with the earlier work from our laboratory suggesting that CD23 associates into trimers (12). These data suggest that at 4°C, the trimer is tightly associated, and only one Ab molecule can bind to it in this form, presumably due to steric hindrance. At 37°C, the trimer partially dissociates, allowing three Ab molecules to bind per trimer, one Ab for each molecule of CD23 in each trimer. Proof that the dissociation is not complete is seen in that Abs that bind to an epitope low on the stalk exhibit the same binding pattern at both high and low temperatures. Thus, only the upper portion of the stalk separates at 37°C, and the lower region of the stalk, near the transmembrane domain, remains tightly associated at all times. Note that these data also fit well with our recent finding that IgE and CD23 interact better at 4 than 37°C and confirm the increased instability of CD23 at physiological temperatures (44). Association of the trimers of CD23 was further investigated using FRET. As discussed above, FRET is the radiationless transfer of energy from an excited fluorophore (donor) to another fluorophore (acceptor). The efficiency of energy transfer is highly dependent on the distance between the donor and the acceptor molecules, and in most cases no FRET is observed at distances >100 Å (38). Recently, a variation of the FRET technique was

described using the green fluorescent protein variants, CFP and YFP, as donor and acceptor molecules, respectively (38, 39). We examined association of CD23 using fusion proteins that contained the fluorescent molecules in-frame at the N terminus. FRET signals from CD23 with CFP and YFP fused to the N terminus (cytoplasmic tail) remained unchanged under all conditions tested, including raising the temperature from 4 to 37°C and addition of the ligand for CD23, IgE. A mutant of CD23 lacking one of the four 21-aa repeats in the stalk (ΔR2) was previously found to bind IgE with only low affinity, presumably because the shortened stalk was no longer able to mediate oligomerization (15). However, we observed the same amount of association with ΔR2 as that with wild-type CD23, suggesting that deletion of the heptad repeats does not interfere with oligomerization, but more likely inhibits the correct conformation of the lectin domains to bind IgE with high affinity. Incubation of cells expressing CD23 with either 19G5 or RAS1, both of which inhibit high affinity IgE binding, did not decrease the FRET signal. This further supports the Ab Scatchard data suggesting that the N terminus remains associated and that only the upper portion of the stalk, including the lectin domains, is mobile. The mobility of the upper stalk region is probably required for the lectin domains to orient themselves in the position required for high affinity IgE binding. These data collectively show that CD23 is preassociated and that association does not require ligand binding. This finding indicates that the earlier model in which monomeric and trimeric CD23 were suggested to be in equilibrium (discussed in Ref. 45) was incorrect. The dissociation apparently only involves the C-terminal portion of the molecule.

A quite novel finding was that the cytoplasmic and transmembrane domains were sufficient for association of CD23. A truncation mutant lacking both the stalk and the lectin domains exhibited the same amount of FRET as wild-type CD23. Although these data do not necessarily bring into question the theory that the stalk region is essential in mediating oligomerization of CD23 (14, 15), they do indicate that the stalk alone is not sufficient. Indeed, the requirement of the transmembrane region, cytoplasmic region, or both for CD23 trimers to form could explain why soluble molecules of CD23 do not readily associate in solution, and indeed, even full-length extracellular CD23 binds IgE only slightly better than sCD23 (13). Previously, our laboratory attached an isoleucine zipper to the extracellular portion of CD23, allowing the soluble form of CD23 (*lz*-ECCD23) to form a stable trimer (34). This molecule bound IgE in a manner similar to that seen with membrane CD23, presumably because the isoleucine zipper enhances trimer formation. These data further confirm the idea that CD23 must form a trimer to bind IgE with high affinity.

These data suggest that the stalks interact with each other only weakly, and the transmembrane region is required for this interaction to proceed efficiently. It is likely that a sequence within the transmembrane region itself is mediating association of the trimers in the membrane and not just the relative immobility of CD23 in the membrane that allows the stalks to interact with each other. The force mediating this interaction is unknown and will be the subject of future investigation by this laboratory. This will include determining whether another protein interacts with the cytoplasmic domain or the transmembrane region of CD23 to mediate the interaction or whether the association is due to direct interactions of the amino acids in the transmembrane region of one CD23 molecule with another molecule of CD23.

In an earlier study we demonstrated the importance of high affinity IgE binding to CD23 in the regulation of IgE production (22). Mice immunized with Ag/alum and treated with the polyclonal anti-stalk Ab exhibited increased serum IgE levels, suggesting that inhibiting oligomerization of CD23, which results in no high affinity IgE binding, leads to dysregulation of IgE production. EBVCS1, an Ab that recognizes the stalk of human CD23, similarly enhances IgE production by stimulated PBMCs (19). An intriguing possibility is that some allergens may increase IgE levels by binding to the stalk of CD23 and interfering with oligomerization. An example of this idea is the cysteine protease, Der p 1, produced by the house dust mite, *Dermatophagoides pteronyssinus.* Der p 1 binds to CD23 and cleaves the stalk region, resulting in increased sCD23 and decreased CD23 surface levels (46–48). Mice injected with Der p 1 produce significantly more total and Ag-specific IgE than mice treated with proteolytically inactive Der p 1 (49), suggesting that the decrease in cell surface CD23 oligomers results in a decrease in regulation of IgE production. These data suggest a potential therapy for IgE-mediated diseases. Stabilization of the trimers on the cell surface could potentially increase high affinity IgE binding and lead to an increase in IgE regulation. Our laboratory is currently examining this idea.

## Acknowledgments

We thank Calvin Wong and Jill Ford for excellent technical support. We also thank Terri Russell and the Virginia Commonwealth University Hybridoma Core Facility for assistance in producing the anti-stalk hybridomas, as well as Ruth Swofford and Jane Clarke of the National Institutes of Health Flow Cytometry Facility for their assistance with flow cytometry.

## References

1. Stief, A., G. Texido, G. Sansig, H. Eibel, G. Le Gros, and H. Van der Putten. 1994. Mice deficient in CD23 reveal its modulatory role in IgE production but no role in T and B cell development. *J. Immunol. 152:3378.*
2. Yu, P., M. Kosco-Vilbois, M. Richards, G. Köhler, M. C. Lamers, and G. Kohler. 1994. Negative feedback regulation of IgE synthesis by murine CD23. *Nature 369:753.*
3. Fujiwara, H., H. Kikutani, S. Suematsu, T. Naka, K. Yoshida, T. Tanaka, M. Suemura, N. Matsumoto, S. Kojima, T. Kishimoto, et al. 1994. The absence of IgE antibody-mediated augmentation of immune responses in CD23-deficient mice. *Proc. Natl. Acad. Sci. USA 91:6835.*
4. Texido, G., H. Eibel, G. Le Gros, and H. Van der Putten. 1994. Transgene CD23 expression on lymphoid cells modulates IgE and IgG1 responses. *J. Immunol. 153:3028.*
5. Payet, M. E., E. C. Woodward, and D. H. Conrad. 1999. Humoral response suppression observed with CD23 transgenics. *J. Immunol. 163:217.*
6. Kehry, M. R., and L. C. Yamashita. 1989. Fcϵ receptor II (CD23) function on mouse B cells: role in IgE dependent antigen focusing. *Proc. Natl. Acad. Sci. USA 86:7556.*
7. Pirron, U., T. Schlunck, J. C. Prinz, and E. P. Rieber. 1990. IgE-dependent antigen focusing by human B lymphocytes is mediated by the low-affinity receptor for IgE. *Eur. J. Immunol. 20:1547.*
8. Keegan, A. D., C. Fratazzi, B. Shopes, B. Baird, and D. H. Conrad. 1991. Characterization of new rat anti-mouse IgE monoclonals and their use along with chimeric IgE to further define the site that interacts with $Fc_{\epsilon}RII$ and $Fc_{\epsilon}RI$. *Mol. Immunol. 28:1149.*
9. Chretein, I., B. Helm, P. Marsh, E. Padlan, J. Wijdenes, and J. Banchereau. 1988. A monoclonal anti-IgE anitbody against an epitope (amino acids 367–376) in the CH3 domain inhibits IgE binding to the low affinity IgE receptor (CD23). *J. Immunol. 141:3128.*
10. Richards, M. L., and D. H. Katz. 1990. The binding of IgE to murine FcϵRII is calcium-dependent but not inhibited by carbohydrate. *J. Immunol. 144:2638.*
11. Sarfati, M., T. Nakajima, H. Frost, E. Kilchherr, and G. Delespesse. 1987. Purification and partial biochemical characterization of IgE-binding factors secreted by a human B lymphoblastoid cell line. *Immunology 60:539.*
12. Rao, M., W. T. Lee, and D. H. Conrad. 1987. Characterization of a monoclonal antibody directed against the murine B lymphocyte receptor for IgE. *J. Immunol. 138:1845.*
13. Bartlett, W. C., A. E. Kelly, C. M. Johnson, and D. H. Conrad. 1995. Analysis of murine soluble FcϵRII: sites of cleavage and requirements for dual affinity interaction with IgE. *J. Immunol. 154:4240.*
14. Beavil, A. J., R. L. Edmeades, H. J. Gould, and B. J. Sutton. 1992. α-Helical coiled-coil stalks in the low-affinity receptor for IgE (FcϵRII/CD23) and related C-type lectins. *Proc. Natl. Acad. Sci. USA 89:753.*
15. Dierks, S. E., W. C. Bartlett, R. L. Edmeades, H. J. Gould, M. Rao, and D. H. Conrad. 1993. The oligomeric nature of the murine FcϵRII/CD23: implications for function. *J. Immunol. 150:2372.*
16. Gould, H., Sutton, B., Edmeades, R., and Beavil, A. CD23/$Fc_{\epsilon}RII$. 1991. C-type lectin membrane protein with a split personality. In *Monographs in Allergy,* Vol. 29, L. A. Hanson and F. Shakib, eds, Karger, Basel, p. 29.
17. Sherr, E., E. Macy, H. Kimata, M. Gilly, and A. Saxon. 1989. Binding the low affinity FcϵR on B cells suppresses ongoing human IgE synthesis. *J. Immunol. 142:481.*

18. Flores-Romo, L., J. Shields, Y. Humbert, P. Graber, J.-P. Aubry, J.-F. Gauchat, G. Ayala, B. Allet, M. Chavez, H. Bazin, et al. 1993. Inhibition of an in vivo antigen-specific IgE response by antibodies to CD23. *Science 261*:*1038.*
19. Wakai, M., P. Pasley, Z. M. Sthoeger, D. N. Posnett, R. Brooks, S. Hashimoto, and N. Chiorazzi. 1993. Anti-CD23 monoclonal antibodies: comparisons of epitope specificities and modulating capacities for IgE binding and production. *Hybridoma 12*:*25.*
20. Nakamura, T., W. S. Kloetzer, P. Brams, K. Hariharan, S. Chamat, X. Cao, M. J. LaBarre, P. C. Chinn, R. A. Morena, W. S. Shestowsky, et al. 2000. In vitro IgE inhibition in B cells by anti-CD23 monoclonal antibodies is functionally dependent on the immunoglobulin Fc domain. *Int. J. Immunopharmacol. 22*:*131.*
21. Yabuuchi, S., T. Nakamura, W. S. Kloetzer, and M. E. Reff. 2002. Anti-CD23 monoclonal antibody inhibits germline Cϵ transcription in B cells. *Int. Immunopharmacol. 2*:*453.*
22. Kilmon, M. A., R. Ghirlando, M. P. Strub, R. L. Beavil, H. J. Gould, and D. H. Conrad. 2001. Regulation of IgE production requires oligomerization of CD23. *J. Immunol. 167*:*3139.*
23. McGrew, J. T., D. Leiske, B. Dell, R. Klinke, D. Krasts, S. F. Wee, N. Abbott, R. Armitage, and K. Harrington. 1997. Expression of trimeric CD40 ligand in *Pichia pastoris*: use of a rapid method to detect high-level expressing transformants. *Gene 187*:*193.*
24. Bazin, H., and A. Beckers. 1976. IgE myelomas in rats. In *Molecular and Biological Aspects of the Acute Allergic Reaction.* S. G. O. Johansson, K. Strandberg, and B. Uvnas, eds. Plenum Press, New York, pp. 125–152.
25. Liu, F.-T., J. W. Bohn, E. L. Ferry, H. Yamamoto, C. A. Molinaro, L. A. Sherman, N. R. Klinman, and D. H. Katz. 1980. Monoclonal dinitrophenyl-specific murine IgE antibody: preparation, isolation, and characterization. *J. Immunol. 124*:*2728.*
26. Isersky, C., A. Kulczycki, Jr., and H. Metzger. 1974. Isolation of IgE from reaginic rat serum. *J. Immunol. 112*:*1909.*
27. Chen, B. H., C. Ma, T. H. Caven, Y. Chan-Li, A. Beavil, R. Beavil, H. Gould, and D. H. Conrad. 2002. Necessity of the stalk region for immunoglobulin E interaction with CD23. *Immunology 107*:*373.*
28. McConahey, P. J., and F. J. Dixon. 1966. A method for trace iodination of proteins for immunologic studies. *Int. Arch. Allergy Appl. Immunol. 29*:*185.*
29. Bazin, H. 1982. Production of rat monoclonal antibodies with the Lou rat non-secreting IR983F myeloma cell line. *Protides Biol. Fluids 29*:*615.*
30. Kohler, G., and C. Milstein. 1975. Continuous cultures of fused cells secreting antibody of predefined specificity. *Nature 256*:*495.*
31. Yu, L. C., G. Montagnac, P. C. Yang, D. H. Conrad, A. Benmerah, and M. H. Perdue. 2003. Intestinal epithelial CD23 mediates enhanced antigen transport in allergy: evidence for novel splice forms. *Am. J. Physiol 285*:*G223.*
32. DeFranco, A. L., E. S. Raveche, R. Asofsky, and W. E. Paul. 1982. Frequency of B lymphocytes responsive to anti-immunoglobulin. *J. Exp. Med. 155*:*1523.*
33. Campbell, K. A., E. J. Studer, M. A. Kilmon, A. Lees, F. D. Finkelman, and D. H. Conrad. 1997. Induction of B cell apoptosis by co-crosslinking CD23 and sIg involves aberrant regulation of c-*myc* and is inhibited by *bcl*-2. *Int. Immunol. 9*:*1131.*
34. Kelly, A. E., B.-H. Chen, E. C. Woodward, and D. H. Conrad. 1998. Production of a chimeric form of CD23 that is oligomeric and blocks IgE binding to the FcϵRI. *J. Immunol. 161*:*6696.*
35. Conrad, D. H., A. D. Keegan, K. R. Kalli, R. Van-Dusen, M. Rao, and A. D. Levine. 1988. Superinduction of low affinity IgE receptors on murine B lymphocytes by lipopolysaccharide and IL-4. *J. Immunol. 141*:*1091.*
36. Siegel, R. M., J. K. Frederiksen, D. A. Zacharias, F. K. Chan, M. Johnson, D. Lynch, R. Y. Tsien, and M. J. Lenardo. 2000. Fas preassociation required for apoptosis signaling and dominant inhibition by pathogenic mutations. *Science 288*:*2354.*
37. Mahajan, N. P., D. C. Harrison-Shostak, J. Michaux, and B. Herman. 1999. Novel mutant green fluorescent protein protease substrates reveal the activation of specific caspases during apoptosis. *Chem. Biol. 6*:*401.*
38. Siegel, R. M., F. K. Chan, D. A. Zacharias, R. Swofford, K. L. Holmes, R. Y. Tsien, and M. J. Lenardo. 2000. Measurement of molecular interactions in living cells by fluorescence resonance energy transfer between variants of the green fluorescent protein. *Sci. STKE 2000*:*L1.*
39. Chan, F. K., R. M. Siegel, D. Zacharias, R. Swofford, K. L. Holmes, R. Y. Tsien, and M. J. Lenardo. 2001. Fluorescence resonance energy transfer analysis of cell surface receptor interactions and signaling using spectral variants of the green fluorescent protein. *Cytometry 44*:*361.*
40. Kenworthy, A. K., and M. Edidin. 1998. Distribution of a glycosylphosphatidylinositol-anchored protein at the apical surface of MDCK cells examined at a resolution of <100 A using imaging fluorescence resonance energy transfer. *J. Cell Biol. 142*:*69.*
41. Lee, W. T., and D. H. Conrad. 1986. Murine B cell hybridomas bearing ligand-inducible Fc receptors for IgE. *J. Immunol. 136*:*4573.*
42. Martin, D. A., L. Zheng, R. M. Siegel, B. Huang, G. H. Fisher, J. Wang, C. E. Jackson, J. M. Puck, J. Dale, S. E. Straus, et al. 1999. Defective CD95/APO-1/Fas signal complex formation in the human autoimmune lymphoproliferative syndrome, type Ia. *Proc. Natl. Acad. Sci. USA 96*:*4552.*
43. Conrad, D. H., and L. H. Peterson. 1984. The murine lymphocyte receptor for IgE. I. Isolation and characterization of the murine B cell Fcϵ receptor and comparison with Fcϵ receptors from rat and human. *J. Immunol. 132*:*796.*
44. Chen, B. H., M. A. Kilmon, C. Ma, T. H. Caven, Y. Chan-Li, A. E. Shelburne, R. M. Tombes, E. Roush, and D. H. Conrad. 2003. Temperature effect on IgE binding to CD23 versus FcϵRI. *J. Immunol. 170*:*1839.*
45. Gould, H. J., B. J. Sutton, A. J. Beavil, R. L. Beavil, N. McCloskey, H. A. Coker, D. Fear, and L. Smurthwaite. 2003. The biology of IgE and the basis of allergic disease. *Annu. Rev. Immunol. 21*:*579.*
46. Schulz, O., P. Laing, H. F. Sewell, and F. Shakib. 1995. Der p I, a major allergen of the house dust mite, proteolytically cleaves the low-affinity receptor for human IgE (CD23). *Eur. J. Immunol. 25*:*3191.*
47. Schulz, O., B. J. Sutton, R. L. Beavil, J. G. Shi, H. F. Sewell, H. J. Gould, P. Laing, and F. Shakib. 1997. Cleavage of the low-affinity receptor for human IgE (CD23) by a mite cysteine protease: nature of the cleaved fragment in relation to the structure and function of CD23. *Eur. J. Immunol. 27*:*584.*
48. Hewitt, C. R. A., A. P. Brown, B. J. Hart, and D. I. Pritchard. 1995. A major house dust mite allergen disrupts the immunoglobulin E network by selectively cleaving CD23: Innate protection by antiproteases. *J. Exp. Med. 182*:*1537.*
49. Gough, L., O. Schulz, H. F. Sewell, and F. Shakib. 1999. The cysteine protease activity of the major dust mite allergen Der p 1 selectively enhances the immunoglobulin E antibody response. *J. Exp. Med. 190*:*1897.*
50. Richards, M. L., D. H. Katz, and F.-T. Liu. 1991. Complete genomic sequence of the murine low affinity Fc receptor for IgE: demonstration of alternative transcripts and conserved sequence elements. *J. Immunol. 147*:*1067* .